Multiparametric optimization of multispectral optoacoustic tomography for deep tissue imaging

Jürgen Glatz, Nikolaos C. Deliolanis, Lu Ding, Adrian Taruttis, Amir Rosenthal, Ralf Schulz, Daniel Razansky and Vasilis Ntziachristos

Chair for Biological Imaging & Institute for Biological and Medical Imaging
Technische Universität München & Helmholtz Zentrum München, Munich, Germany

ABSTRACT

Over the last decade fluorescent reporter technologies (both fluorescent probes and proteins) have become a very powerful imaging tool in everyday biomedical research. Multispectral optoacoustic tomography (MSOT) is an emerging imaging technology that can resolve fluorophore concentration in small animals situated in deep tissue by multispectral acquisition and processing of optoacoustic signals. In this work, we study the optimum operating conditions of MSOT in imaging fluorescence activity in small animals. The performance of various fluorochromes / fluorescent proteins is examined and it is shown that the new infrared fluorescent protein is an order of magnitude brighter than the red ones. Finally, wavelength reduction after principle component analysis shows, that accurate unmixing and 3D reconstruction of the distribution of fluorochromes is possible only with 2 or 3 wavelengths.

Keywords: multispectral, fluorescent protein, photoacoustic, tomography, molecular imaging

1. INTRODUCTION

Optoacoustic imaging is a hybrid biomedical imaging technique that incorporates the advantages of optical and ultrasound imaging, while overcoming their respective limitations. When tissue is illuminated with short laser pulses, light gets absorbed and causes topical thermal expansion followed by contraction when the pulse subsides.[1] This movement creates an acoustic pressure wave that propagates within the tissue and can be detected by an ultrasonic transducer. The easy propagation of ultrasound waves through tissue, long-standingly used in ultrasound imaging, allows for a high spatial resolution and penetration depth. Additionally, optoacoustic imaging - unlike ultrasonography - offers good contrast, due to tissue absorption. In photoacoustic tomography (PAT) the generated pressure wave is recorded at multiple detector positions and by means of computed tomography the three-dimensional map of absorption is reconstructed. An advantage of PAT is that it uses non-ionizing radiation, as opposed to X-ray CT and positron emission tomography, which is not harmful to biological tissue in the recommended intensities. For this, optoacoustic imaging is a highly promising modality for noninvasive and in vivo deep tissue imaging applications.

In the past decade, the usage of the fluorescent proteins (FPs) in everyday lab work has revolutionized biomedical discovery. They have been used in many research areas, such as cancer research[2] and drug discovery[3] to visualize functional and molecular processes. The green fluorescent protein[4] (GFP) and its cyan (CFP) and yellow (YFP) emitting mutations are commonly used, but their applicability in deep tissue imaging is restricted by the relatively strong tissue absorbance in this spectral region. However, the efforts of protein engineers have led to the introduction of a new generation of proteins, that absorb and emit in the red spectral range[5–8] or the near infrared range[9] .

Further author information:
Nikolaos Deliolanis (E-Mail: n.deliolanis@helmholtz-muenchen.de
Helmholtz Zentrum München, GmbH
Ingolstädter Landstraße 1
85764 Neuherberg, Germany

Photons Plus Ultrasound: Imaging and Sensing 2010, edited by Alexander A. Oraevsky, Lihong V. Wang,
Proc. of SPIE Vol. 7564, 75642Z · © 2010 SPIE · CCC code: 1605-7422/10/$18 · doi: 10.1117/12.842101

Fluorophores and fluorescent proteins have been widely imaged with conventional and confocal fluorescent microscopy, as well as other macroscopic imaging methods, but it was recently shown[10,11] that such fluorescent markers can also be employed for photoacoustic imaging, using their absorption. The key to this is multispectral optoacoustic tomography (MSOT), in which the specimen is excited at several wavelengths and the fluorophore signals are unmixed against the tissue background using its known absorption spectrum. In this work we evaluate the performance of different fluorophores for use with MSOT in deep tissue imaging applications and demonstrate the optimal parameters for spectral measurement and unmixing.

2. COMPARISON OF THE PERFORMANCE OF VARIOUS FLUORESCENT PROTEINS

In order to compare the photoacoustic pressure produced from the various fluorescent proteins in deep tissue, we employ a simple light propagation model. As shown in Figure 1, the optoacoustic signal formation can be divided into two parts. Firstly the light path, describing the propagation of the laser pulses through the tissue to the fluorochromes and secondly the acoustic path, describing the acoustic wave propagation.

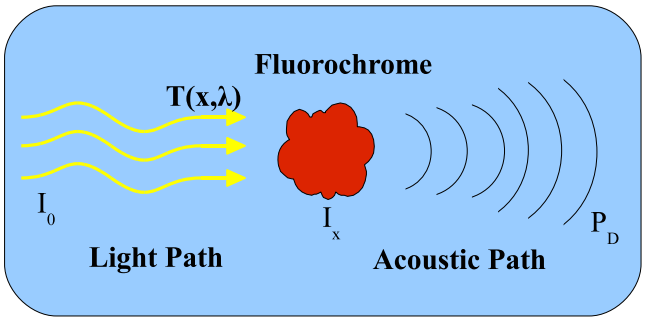

Figure 1: Illustration of the simple photon propagation model

The light intensity that reaches a protein at a depth x is denoted by $I_x = T(x,\lambda)I_0$. Thereby λ and I_0 are the laser wavelength and intensity while $T(x,\lambda)$ is the tissue relative spectral transmittance for thickness x and wavelength λ. The ultrasonic signal amplitude at the detector can be calculated as $P_D \propto (1-\Phi)\varepsilon I_x$, yielding

$$P_D \propto (1-\Phi)\varepsilon T(x,\lambda)I_0$$

for the detected signal intensity, where Φ is the quantum yield and ε is the molar extinction coefficient. Substituting the spectral transmission of 8 mm mouse tissue from *in vivo* measurements[12] and the optical characteristics of the FPs[6,7,9] (see Fig. 2a) we get the spectral photoacoustic pressure shown in Fig. 2b. The calculated photoacoustic signal produced by IFP is more than one order of magnitude stronger than that of mRaspberry (the most absorbing of the RFPs) and more than 3 orders of magnitude stronger than GFP. All three proteins have molar extinction coefficients that fall in the 50000-10000 cm^{-1} range and it is the low tissue absorption in the far-red part of the spectrum that results in the superior performance of IFP.

3. SIMULATION STUDY

The performance of the three fluorescent proteins GFP, mRaspberry and IFP in MSOT was analyzed with a simulation study. The simulated object is a small protein inclusion of 1.2 mm diameter in the cervical region of a mouse. Based on transfection levels reported in the literature,[4] the proteins were assumed to have a concentration of 1 μM each. Biological tissue is characterized by its strong optical scattering and therefore referred to as a turbid medium. Scattering events are assumed to be elastic and the illuminating light is considered to be monochromatic and unpolarized for the subsequent model. Generally, the radiative transfer equation can be solved numerically with Monte Carlo simulations[13,14] if the object's optical properties are known.

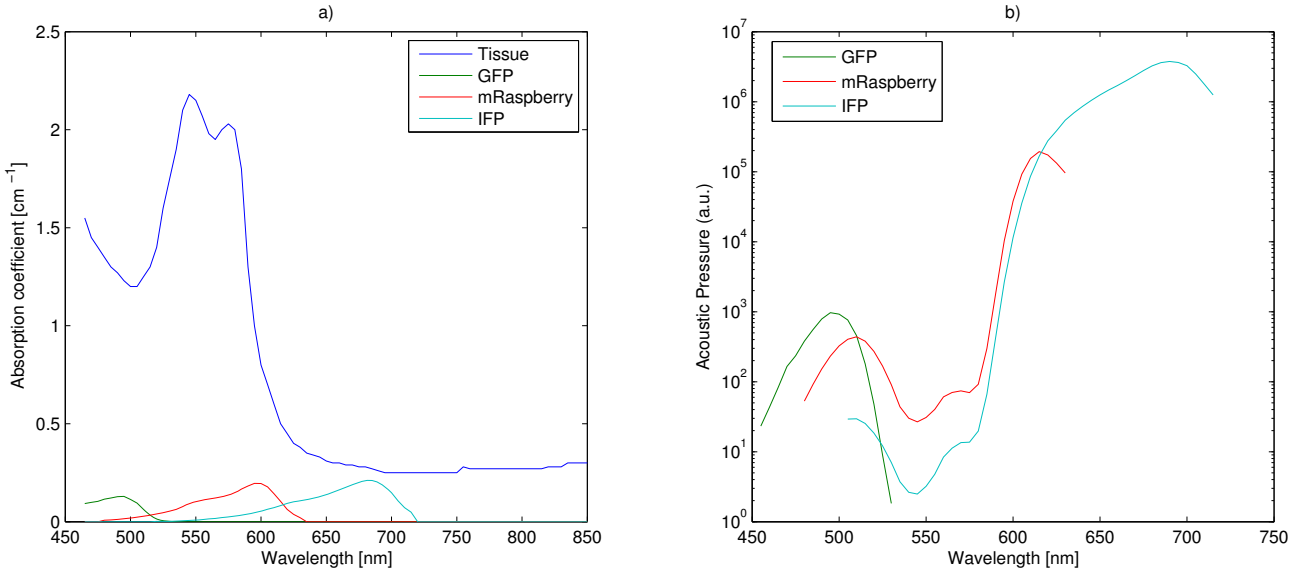

Figure 2: a) Absorption spectrum for tissue background and fluorescent proteins. b) Estimated photoacoustic pressure of proteins in arbitrary units

In this work, however, the diffusion approximation is used and solved by a finite-element-based inversion.[15] The average absorption coefficients of tissue and the protein inclusions are shown in Fig. 2a. In order to reconstruct the image from the simulated acoustic measurements the filtered backprojection algorithm for photoacoustic tomography[16] is employed. It should be noted that backprojection only yields an image of the photoacoustic pressure distribution and not a map of the original optical absorption. The actual optical properties can be obtained by correcting the resulting photoacoustic image for the light distribution within the object.[17] The acoustic signals were simulated for wavelengths from 465 - 720 nm in steps of 5 nm and for 180 angular projections. Additive gaussian noise was added to obtain realistic conditions. After reconstructing with backprojection, a correction for the light attenuation was applied by dividing the images with the photon propagation distribution in the tisse and the obtained images were unmixed with independent component analysis[18] (ICA), as shown in Figure 3. For the unmixing, the measurements at three wavelengths were used for each protein. The optimal wavelength selection was determined from a principal component analysis (PCA) of the reconstructed data, choosing the wavelengths corresponding best to the primary components. It can be seen that the results are consistent with the photoacoustic pressure estimation given in Figure 2b. GFP can barely be unmixed from the noise, mRaspberry gives a slightly stronger signal and IFP clearly performs best, being easily distinguishable.

4. DISCUSSION AND CONCLUSIONS

Switching to the new red-shifted FPs and utilizing optimum excitation wavelengths has increased the signal intensity up to 2-3 orders of magnitude compared to GFP, depending on the particular geometry of the problem. Using a brighter fluorescent protein, like IFP would be an improvement of a factor of 4. However, a key element in the successful unmixing of signals is the correction for the light attenuation by calculating the light propagation in tissue. Since in most spectral regions the optical properties of tissue are wavelength-dependent, the correct spectral modeling of light propagation is essential for the correct unmixing.

In this paper, we have studied a multi-spectral optoacoustic tomographic scheme that allows the accurate reconstruction of FP activity located deep inside tissue, employing optimum illumination and efficient unmixing techniques. The palette of FPs working in the 590-630 nm excitation-emission peak range is already complete and the development of new FPs that work in the near IR will boost the detected signal intensity.

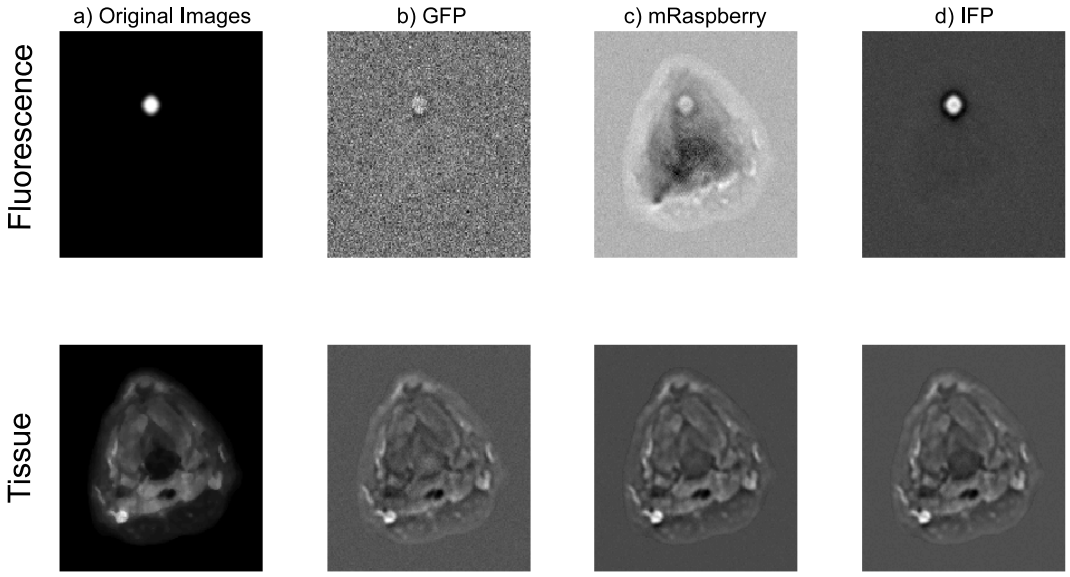

Figure 3: a) Simulated protein distribution and tissue background; ICA unmixing for b) GFP, c) mRaspberry and d) IFP

ACKNOWLEDGMENTS

This research is supported by a Marie Curie Intra-European Fellowship within the 7th European Community Framework.

REFERENCES

[1] Bowen, T., "Radiation-induced thermoacoustic soft tissue imaging," in [*Ultrasonics Symposium*], (2), 817–822, IEEE (1981).

[2] Hoffman, R., "The multiple uses of fluorescent proteins to visualize cancer in vivo," *Nature Reviews Cancer* **5**, 796–806 (October 2005).

[3] Licha, K. and Olbrich, C., "Optical imaging in drug discovery and diagnostic applications," *Advanced Drug Delivery Reviews* **57**(8), 1087 – 1108 (2005).

[4] Tsien, R. Y., "The green fluorescent protein," *Annual Review of Biochemistry* **67**(1), 509–544 (1998).

[5] Matz, M. V., Fradkov, A. F., Labas, Y. A., P., S. A., Zaraisky, A. G., Markelov, M. L., and Lukyanov, S. A., "Fluorescent proteins from nonbioluminescent anthozoa species," *Nature Biotech* **17**, 969–973 (October 1999).

[6] Shaner, N. C., E., C. R., Steinbach, P. A., Giemans, B. N. G., Palmer, A. E., and Tsien, R. Y., "Improved monomeric red, orange and yellow fluorescent proteins derived from discosoma sp. red fluorescent protein," *Nature Biotech* **22**, 1567–1572 (December 2004).

[7] Shaner, N. C., Steinbach, P. A., and Tsien, R. Y., "A guide to choosing fluorescent proteins," *Nature Methods* **2** (December 2005).

[8] Shcherbo, D., Murphy, C. S., Ermakova, G. V., Solovieva, E. A., Chepurnykh, T. V., Shcheglov, A. S., Verkhusha, V. V., Pletnev, V. Z., Hazelwood, K. L., Roche, P. M., Lukyanov, S., Zaraisky, A. G., Davidson, M. W., and Chudakov, D. M., "Far-red fluorescent tags for protein imaging in living tissues," *Biochemical Journal* **418**(3), 567–574 (2009).

[9] Shu, X., Royant, A., Lin, M. Z., Aguilera, T. A., Lev-Ram, V., Steinbach, P. A., and Tsien, R. Y., "Mammalian expression of infrared fluorescent proteins engineered from a bacterial phytochrome," *Science* **324**(5928), 804–807 (2009).

[10] Razansky, D., Vinegoni, C., and Ntziachristos, V., "Multispectral photoacoustic imaging of fluorochromes in small animals," *Optics Letters* **32**(19), 2891–2893 (2007).

[11] Razansky, D., Distel, M., Vinegoni, C., Ma, R., Perrimon, M., Koster, R. W., and Ntziachristos, V., "Multispectral opto-acoustic tomography of deep-seated fluorescent proteins in vivo," *Nature Photonics* **3**, 412–417 (July 2009).

[12] Deliolanis, N. C., Kasmieh, R., Wurdinger, T., Tannous, B. A., Shah, K., and Ntziachristos, V., "Performance of the red-shifted fluorescent proteins in deep-tissue molecular imaging applications," *Journal of Biomedical Optics* **13**(4), 044008 (2008).

[13] Wang, L. V. and Jacques, S. L., "Hybrid model of monte carlo simulation and diffusion theory for light reflectance by turbid media," *Journal of the Optical Society of America A* **10**(8), 1746–1752 (1993).

[14] Prahl, S. A., Keijzer, M., Jacques, S., and Welch, A. J., "A monte carlo model of light propagation in tissue," in [*SPIE Proceedings of Dosimetry of Laser Radiation in Medicine and Biology*], Mller, G. and Sliney, D., eds., **5**, 102–111 (1989).

[15] Razansky, D. and Ntziachristos, V., "Hybrid photoacoustic fluorescence molecular tomography using finite-element-based inversion," *Medical Physics* **34**(11), 4293–4301 (2007).

[16] Xu, M. and Wang, L. V., "Universal back-projection algorithm for photoacoustic computed tomography," *Phys. Rev. E* **71**, 016706 (Jan 2005).

[17] Jetzfellner, T., Razansky, D., Rosenthal, A., Schulz, R., Englmeier, K.-H., and Ntziachristos, V., "Performance of iterative optoacoustic tomography with experimental data," *Applied Physics Letters* **95**(1), 013703 (2009).

[18] Hyvrinen, A., Karhunen, J., and Oja, E., [*Independent Component Analysis*], Adaptive and Learning Systems for Signal Processing, Communications, and Control, Wiley InterScience, 1st edition ed. (May 2002).